NJC

Accepted Manuscript

This is an *Accepted Manuscript*, which has been through the Royal Society of Chemistry peer review process and has been accepted for publication.

Accepted Manuscripts are published online shortly after acceptance, before technical editing, formatting and proof reading. Using this free service, authors can make their results available to the community, in citable form, before we publish the edited article. We will replace this *Accepted Manuscript* with the edited and formatted *Advance Article* as soon as it is available.

You can find more information about *Accepted Manuscripts* in the Information for Authors.

Please note that technical editing may introduce minor changes to the text and/or graphics, which may alter content. The journal's standard Terms & Conditions and the Ethical guidelines still apply. In no event shall the Royal Society of Chemistry be held responsible for any errors or omissions in this *Accepted Manuscript* or any consequences arising from the use of any information it contains.

ROYAL SOCIETY OF CHEMISTRY

www.rsc.org/njc

Journal Name

ARTICLE

Planar and Distorted Indigo as Core Motif in Novel Chromophoric Liquid Crystals

Received 00th January 20xx,
Accepted 00th January 20xx

DOI: 10.1039/x0xx00000x

www.rsc.org/

Jan H. Porada,[a,b] Jörg Neudörfl[a] and Dirk Blunk[a]*

Symmetrically bis-substituted indigo derivatives with long peripheral alkyl chains were synthesised by reductive condensation of corresponding isatin derivatives. Their thermotropic mesomorphism was investigated with respect to different substitution patterns, including position and lateral modifications of the substituents. A systematic investigation of structure-property relationships revealed that only substitution at the 6,6′ positions affords the calamitic shape necessary to form smectic or nematic liquid crystalline phases. This finding is rationalised on the basis of a structural analysis of *N,N*′-diacetyl indigo and the consequences for 5,5′- and 6,6′-bis-substituted derivatives. Some of the liquid crystalline substances exhibit dichroism, which is especially pronounced in highly ordered phases. Additionally, the 6,6′ substitution leads to a significantly enhanced activity concerning the photochemical trans-cis isomerization of the *N,N*′-diacetylated indigo derivatives.

Introduction

The spatial anisotropic alignment of chromophores is an essential requirement for many high-tech applications in which a macroscopic directed effect is generated by interaction of light and matter. Examples can be found in the field of non-linear optics,[1] organic photovoltaics,[2] laser technology[3] or supramolecular photo-chemistry.[4] Due to the rather small HOMO-LUMO gap, which causes the colour of the chromophore, further applications in the field of molecular electronics are possible.[5] Common methods of approaching the challenge of molecular alignment are shown in Figure 1 and described below. They are:

a) Embedding a chromophoric guest in an anisotropic **host matrix**. Such a matrix usually consists of low molecular weight or polymeric liquid crystals or polymers which have been aligned by stretching or even oriented in a polar order by various poling techniques.[1b, c] Field induced switching of the chromophore orientation can be achieved by choosing a polar matrix[6] or an appropriate LC cell geometry.[7]

b) Covalent integration of a chromophoric substructure into the side-chains of a polymer backbone (**side-chain** polymers).[1b, c, 8] Such side-chain polymers are often designed to have liquid-crystalline properties.[1a]

c) Polymerization of chromophoric monomers to a **main-chain** polymer or copolymer.[1b, 9]

d) the **structural integration** of the chromophore into a molecular framework of a low molecular weight anisometric molecule, capable of forming a liquid crystalline phase.[10] This method is by far the least common but nevertheless a very promising approach.

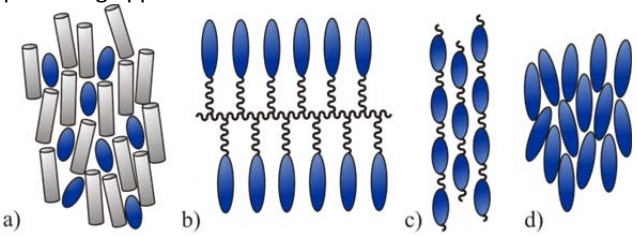

Figure 1. Possible methods to align chromophores.

The latter method (d) leads to materials with a significantly higher chromophore density then host-guest-systems (a) without the possibility of phase separation or physical demixing. In contrast to polymers (b) or (c), the product can be synthesized and purified in a precise manner. The presumably higher solubility of such chromophoric mesogens compared to polymeric systems would be advantageous for technical applications.

In this context indigo seemed to be a suitable chromophoric molecular core as a starting point for the design of colored mesogens. This is not only due to its rather small chromogenic motif and its high thermal and photochemical stability, but also to the C_{2h}-symmetry of the indigo molecule. Due to the

[a] *Dr. Jan H. Porada, Dr. Jörg Neudörfl, Dr. Dirk Blunk*
Universität zu Köln, Institut für Organische Chemie
Greinstr. 4, 50939 Köln (Germany)
E-mail: d.blunk@uni-koeln.de – Fax: (+49) 221-470 3064
Homepage: www.oc.uni-koeln.de/blunk
[b] *Dr. Jan H. Porada,*
Universität Stuttgart, Institut für Physikalische Chemie
Pfaffenwaldring 55, 70569 Stuttgart (Germany),

Electronic Supplementary Information (ESI) available: [A description of the experimental details, the analytical data, UV-Vis spectra, the calculations of the order parameters, π-orbital axis vectors and DFT calculations is given. CCDC 1033834 (**12**) and CCDC 811039 (**23**) contain the supplementary crystallographic data for this paper. These data can be obtained free of charge from The Cambridge Crystallographic Data Center via http://www.ccdc.cam.ac.uk/data_request/cif.]. See DOI: 10.1039/x0xx00000x

latter, it can easily be substituted in a symmetric way generating rod-like molecules. Furthermore many synthetic approaches towards indigo and its analogues – including donors like selenium, sulphur or oxygen – are known, which will give broad access to a wide structural diversity of suitable molecules. Once the basic structure-property relations are studied, a desymmetrisation by corresponding synthetic strategies can broaden the structural diversity and give access to polar mesophases.

Despite the fact that indigo was intensely studied since the end of the 19th century, the reason for its remarkably low frequency absorption (indicating its small HOMO-LUMO gap) was inscrutable for decades. It was only in the 1960s that quantum mechanical calculations revealed that the biggest contribution to the chromophoric properties originates from the double-crossed donor-acceptor substructure, which is formed by the vinylogue amides. The aromatic rings contribute to the chromophoric system mainly by stabilizing the coplanar conformation of the molecule and only marginally by mesomeric effects.[11] The position of the absorption maximum can be fine-tuned by the type of the peripheral substituents.[12]

Here we present our results concerning the synthesis and the thermotropic properties of a variety of symmetrically bis-substituted indigo derivatives.

Results and Discussion

Synthesis

The structural requirements for mesogenic behaviour were established by the introduction of pendant groups with long aliphatic chains at the lateral positions of the phenyl rings of the indigo unit. Though numerous synthetic approaches to indigo are known, most of them are inadequate for the synthesis of complex derivatives, due to their aqueous reaction conditions which are incompatible with the extended aliphatic moieties of the pendant groups. An exception which employs organic solvents, is the reaction of isatin (1) with phosphorus pentachloride in benzene and the subsequent reductive condensation of the resulting 2-chloro-3*H*-indole-3-one (2), finally using zinc dust or hydrogen iodide as reducing agent to yield indigo (3) with varying amounts of indirubin as by-product. Actually, this procedure was one of the first indigo syntheses and was described by Baeyer in 1879.[13] The formation of indirubin can be avoided by applying refined reductive conditions, i.e. using thiophenol as the reducing agent in benzene (Scheme 1) under inert atmosphere as published by Katritzky *et al.*[14]

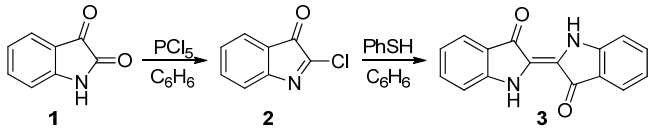

Scheme 1. Synthesis of indigo (**3**) with thiophenol as mild reducing agent performed in an organic solvent, as published by Katritzky.[14]

A modified one pot methodology was developed using the less toxic toluene as solvent to transform substituted isatin derivatives of type **B** into the corresponding indigo derivatives of type **C** (Scheme 2). This procedure was also applied successfully with respect to the synthesis of analogue structures in our previous publication about phasmidic indigo derivatives.[15] The pendant groups were introduced via Suzuki-Miyaura coupling of the bromoisatins of type **A** (Scheme 2) with the corresponding boronic acid of the pendant groups **4-7**.[16]

For further diversification and to suppress the formation of hydrogen bonds, which are known to cause the high melting temperature of pure indigo,[17] the vinylogue amide functions were masked by acetylation, affording the indigo derivatives of type D (Scheme 2). The acetylation method published by Liebermann and Dickhut using acetic anhydride as solvent,[18] while reactive towards indigo did not result in any conversion. Also, when using polar aprotic solvents, conversion could be observed in NMP, but not in DMF or DMSO. The origin of this effect is not completely understood, yet. The whole sequence, starting from the boronic acids **4-7** and bromoisatines A is shown in Scheme 2.

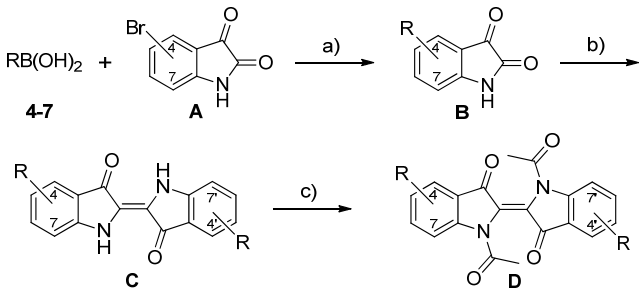

Scheme 2. General synthetic route to the symmetrically bis-substituted indigo derivatives of type C and D. a) K_3PO_4 (aq, 2 eq), $Pd(PPh_3)_4$ (2 mol%), DME, 90°C; b) 1. PCl_5 (1.05 eq), 2. PhSH (2.2 eq), toluene, 100°C; c) $AcCl/Ac_2O$, NMP, 90°C.

In order to evaluate the influence of the pendant groups on mesomorphic behaviour, four boronic acids **4-7**, shown in Figure 2, were employed. Those differ in the chain type being an alkyl- (**4**) or alkoxy-chain (**5-7**) or in a lateral substitution of the substituent with a fluorine atom (**6**) or a methyl group (**7**).

While **4-6** were synthesised according to published procedures[15, 19] the 4-dodecyloxy-2-methyl-phenyl boronic acid (**7**) was obtained by selective bromination of the 4-position of *m*-cresole in acetonitrile,[20] followed by etherification with bromododecane and treatment with *n*-butyl lithium and trimethylborate and subsequent acidic workup.

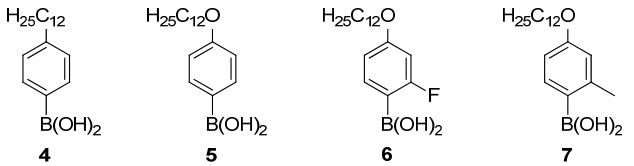

Figure 2. The boronic acids of the employed pendant groups **4-7**.

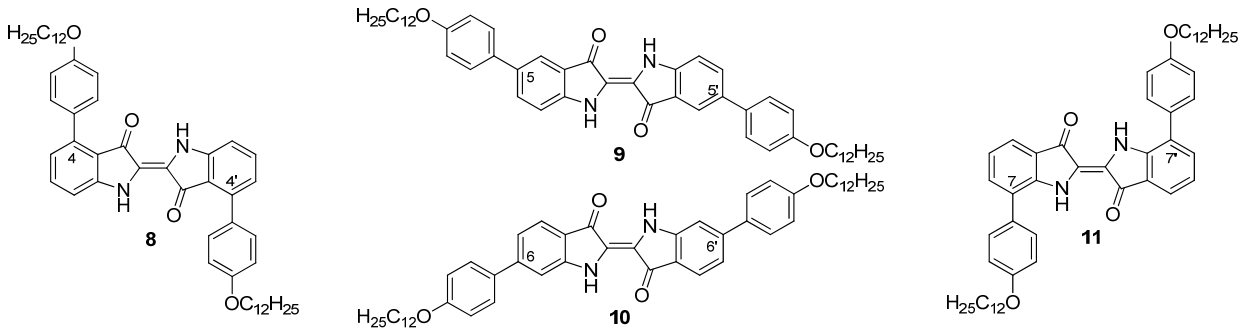

Figure 3. The four symmetrically 4-dodecyloxyphenyl-bissubstituted indigo-derivatives 8-11.

Mesomorphic Properties

The symmetrically substituted compounds of type **C** were investigated, in order to observe how shape anisotropy affected the mesogenic properties of bis-substituted indigo derivatives.

The four resulting regioisomeric 4-dodecyloxyphenyl-bissubstituted indigo-derivatives **8**-**11** are shown in Figure 3. Their thermotropic behaviour was investigated by polarization microscopy (PM) and differential scanning calorimetry (DSC) and is summarized in Table 1.

Table 1. Thermal data[a] of the four symmetrically 4-dodecyloxyphenyl-bissubstituted indigo-derivatives 8-11 shown in Figure 3.

	Cr		●		I
8	●	— / —	—	253 / 251.1 (37.6)	●
9	●	350 / 348	SmX	Decomposition	—
10	●	325 / 320	—	Decomposition	—
11	●	— / —	—	217 / 218.2 (30.1)	●

[a] Form of designation: PM / DSC [°C] (ΔH [kJ/mol]), SmX: smectic phase of unknown type.

As seen from Table 1, compounds **8** and **11** show a direct transition from crystal to isotropic liquid, whereas the compounds **9** and **10** melt at much higher temperatures, while undergoing decomposition. Shortly before decomposition of compound **9**, a fan-like texture, indicating a smectic phase, was observed by PM. Further characterization of the phase was not possible, due to decomposition. The different melting behaviour of these four compounds can be rationalized with regard to the role of the hydrogen bonds. It can be assumed that **9** and **10** form a hydrogen bond network, similar to indigo[17] which causes the high melting temperatures. In compounds **8** and **11** these intermolecular H-bonds are sterically hindered by the 4-dodecyloxy substituents, which leads to a significant reduction of the melting temperatures. This interpretation is supported by the fact that **8** and **11** exhibit unusual high solubility in solvents as chloroform, whereas **9** and **10** only form colloidal suspensions in chloroform.

Due to their rod like molecular shape the indigo derivatives **9** and **10** seemed to have the most promising structural motifs for designing liquid crystalline compounds. To overcome the high melting temperatures the vinylogue amide functions were masked by acetylation leading to the diacetylated compounds **12** and **13** shown in Figure 4. The introduction of methyl groups as possible alternative was not performed, because the dimethyl indigo is known to exhibit a low thermal stability and readily oxidizes to the methyl isatin[21]

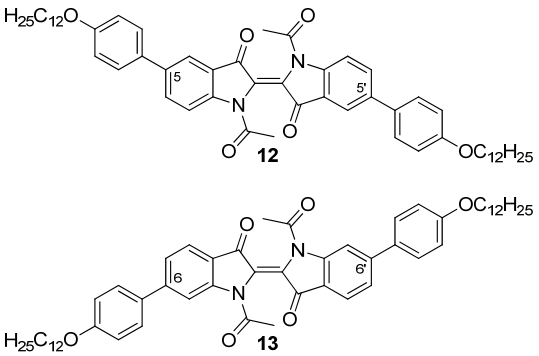

Figure 4. The *N,N'*-diacetylated indigo derivatives with 4-dodecyloxyphenyl pendant groups in positions 5,5' (**12**) or 6,6'(**13**).

With compound **12** and **13** a dramatic reduction of the melting temperatures, accompanied by an increase of the solubility was achieved with respect to their parent compounds **9** and **10**, respectively.

Table 2. Thermal data[a] of the *N,N'*-diacetylated indigo derivatives **12** and **13** shown in Figure 4.

	Cr		●		I
12	●	127 / 124.8 (53.2)[b]	SC	162 / 160.5 (26.7)	●
13	●	181 / 180.6 (10.7)	SmA	201 / 203.9 (7.0)	●

[a] Form of designation: PM / DSC [°C] (ΔH [kJ/mol]), [b] could only be observed in the first heating cycle, SC: soft crystalline phase, SmA: smectic A phase.

Upon heating, **12** undergoes a phase transition at 124.8°C into a soft crystalline phase SC which could only be observed on first heating. At 160.5°C this SC phase melts into the isotropic liquid. Compound **13** shows a phase transition at 180.6°C into the SmA phase, as determined by PM. The phase grows from the isotropic melt as bâtonnets, which finally converge into a fan like texture. Upon shearing homeotropic alignment could be achieved. By conoscopy a uniaxial, optical positive character was identified, which is in accordance with an orientation of the molecular long axis perpendicular to the layers and parallel to the viewing axis.

In addition to our previously published phasmidic indigo derivatives, **13** now represents the first example of a calamitic liquid crystal that possesses an indigo core. To gain insight into the effect of different pendant groups on the mesomorphic behaviour, the structures summarized in Figure 5 were examined. The influence of the oxygen atom in the alkoxy chain was evaluated by comparison to analogue alkyl derivatives bearing no oxygen. Then the effect of lateral substituents on the pendant groups was investigated. A differentiation between electronic and steric effects was achieved by using fluorine or methyl groups as the lateral substituent. The thermal data of these compounds are presented in Table 3. The influence of the four varied parameters, i.e. the substitution positions, the *N*-substituent R1, the chain type R2 and the lateral substituent X (see Figure 5) will be discussed in the following part. In this discussion the main subdivisions are given at first by the substitution positions and after that by the *N*-substituent R1.

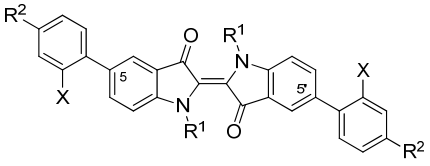

9 (R^1=H, R^2= $OC_{12}H_{25}$, X=H)
14 (R^1=H, R^2= $C_{12}H_{25}$, X=H)
15 (R^1=H, R^2= $OC_{12}H_{25}$, X=F)
16 (R^1=H, R^2= $OC_{12}H_{25}$, X=Me)
12 (R^1=Ac, R^2= $OC_{12}H_{25}$, X=H)
17 (R^1=Ac, R^2= $C_{12}H_{25}$, X=H)
18 (R^1=Ac, R^2= $OC_{12}H_{25}$, X=F)
19 (R^1=Ac, R^2= $OC_{12}H_{25}$, X=Me)

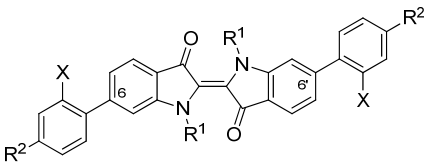

10 (R^1=H, R^2= $OC_{12}H_{25}$, X=H)
20 (R^1=H, R^2= $C_{12}H_{25}$, X=H)
21 (R^1=H, R^2= $OC_{12}H_{25}$, X=F)
22 (R^1=H, R^2= $OC_{12}H_{25}$, X=Me)
13 (R^1=Ac, R^2= $OC_{12}H_{25}$, X=H)
23 (R^1=Ac, R^2= $C_{12}H_{25}$, X=H)
24 (R^1=Ac, R^2= $OC_{12}H_{25}$, X=F)
25 (R^1=Ac, R^2= $OC_{12}H_{25}$, X=Me)

Figure 5. Compilation of the substitution patterns of the synthesised indigo derivatives with pendant groups in the positions 5,5′ or 6,6′ and *N,N*′-disubstitution, respectively.

For the 5,5′-bis-substituted indigo derivatives a direct comparison between the *N,N*′-unsubstituted compounds **9** and **14** differing only by an oxygen atom in the chain reveals a minor stabilization of the crystalline phase, caused by the alkoxy oxygen. Upon introduction of lateral fluorinated pendant groups of compound **15** the formation of a second crystalline phase Cr2 was observed at 116.8°C, which decomposes at 320°C, forming a smectic phase while decomposing, also observed in the compound **9**. The laterally methylated pendant groups of **16** reduce the stability of the crystalline phase of the *N,N*′-unsubstituted compound enough to melt, without decomposition, into an isotropic phase after transitioning through a soft crystalline phase SC.

The mesomorphic behaviour of *N,N*′-diacetylated compounds **12** and **17** differ clearly with respect to each other. The soft crystalline phase SC, which was found in **12** cannot be detected in compound **17**. Further, the melting point is reduced by 53°C with respect to **12** and solidifies as an isotropic glass. For the corresponding laterally fluorinated compound **18** a stabilization of the crystalline phase by 10°C could be observed compared to **12**.

The laterally methylated analogue **19**, much like **17**, shows significant destabilization of the crystalline phase by approximately 50°C with respect to **12**. None of the 5,5′-bis-substituted, *N,N*′-diacetylated compounds possess liquid crystalline phases.

Table 3. Thermal data of the indigo derivatives shown in Figure 5.

		Cr	●		●		I
14	●	— / —	—	345/341	SmX	Decomposition	—
15	●	— /116.6 (38.3)	Cr_2	320/322.9 (36.5)	SmX	Decomposition	—
16	●	— / —	—	— /241.4 (4.4)	SC	266/268.6 (56.6)	●
17	●	— / —	—	— / —	—	108/106.8 (56.2)[b, c]	●
18	●	— / —	—	— / —	—	169/170.9 (32.6)	●
19	●	— / —	—	— / —	—	110/110.6 (47.2)	●
20	●	— / —	—	288/ —	—	Decomposition	—
21	●	— /165.8 (13.7)	Cr_2	— /239.2 (7.9)	SmF/I	295/296.8 (56.1)	●
22	●	— / —	—	— /141.0 (20.5)	SmF/I	261/263.8 (44.2)	●
23	●	— /99.2 (18.8)	SC_2	172/168.1 (7.6)	SmA	176/178.0 (6.9)[d]	●
24	●	141/140.7 (15.5)	SmA	145/145.9 (1.3)	N	149/149.3 (1.9)	●
25	●	— / —	—	— / —	—	199/198.0 (50.3)	●

[a] Form of designation: PM / DSC [°C] (ΔH [kJ/mol]), [b] could only be observed in the first heating cycle, [c] solidifies as amorphous glass, [d] values from cooling cycle, Cr: crystalline phase, SmX: smectic phase of unknown type, SC: soft crystalline phase, SmF/I: smectic F or smectic I phase, SmA: smectic A phase, N: nematic phase.

The 6,6′-bis-substituted indigo derivatives already show clear differences at the *N,N*′-unsubstituted stage, in contrast to the 5,5′-bis-substituted derivatives. Compared to the bis-alkoxyphenyl substituted compound **10**, the bis-alkylphenyl substituted compound **20** shows a reduction of the melting temperature by approx. 30°C, but decomposition still occurs. For both, the *N,N*′-unsubstituted laterally fluorinated compound **21** and especially the lateral methylated compound **22** a decrease in stability of the crystalline phase in comparison to **10** and the formation of a high order liquid crystalline phase were observed. While the decrease of the crystal phase stability is approximately 80°C for the fluorinated compound **21**, it is 180°C for the methylated analogue **22**. Both compounds clear into the isotropic phase without decomposition. The liquid crystalline phase found for **21** and **22** was assigned either to be of SmI or SmF type, based upon the following observations:

Shearing is possible, but the high resistance indicates a high degree of molecular order. Furthermore, the high transition

enthalpies of the liquid crystal to isotropic transition support this assumption.

The phase growth from the isotropic melt is dendritic, as is typically observed for highly ordered phases.

A smectic phase is more reasonable than a columnar one, due to the particular molecular shape and the non-curved polar/apolar-interface of these compounds.

Conoscopy revealed an optical biaxial character in each domain. An orientation of the bisectrix parallel or orthogonal to the viewing axis could be excluded. Such an orientation cannot be explained without assuming an intrinsic tilt of the molecules with respect to the layer normal. Therefore a SmB-phase can be excluded.

Evidently, the bis-substitution in the positions 6 and 6′ has a greater influence on the phase behaviour compared to bis-substitution in the positions 5 and 5′. Depending on the 6,6′-bis-substituent the stability of the crystal phase can be reduced tremendously. An explanation could be that sterically demanding substituents in these positions cause a change of the H-bond network. The three dimensional network, known from indigo,[17] in which each molecule is connected with each one H-bond to four other molecules oriented perpendicular is given up in favour to strands where each molecule is connected by two H-bonds to two others in parallel orientation. As a result of such uniform alignment of light absorbing molecules a pronounced dichroism should be observed, which was found for the 6,6′-bis-substituted indigo derivatives **21** and **22** in the LC phase. Figure 6 shows the UV-Vis-absorption spectra of **22** with two maxima in the visible range. The absorption at 604 nm causes a blue visual impression, whereas absorption at 398 nm relates to a yellow colour. Indeed, as consequence of the superposition, the substance appears green.

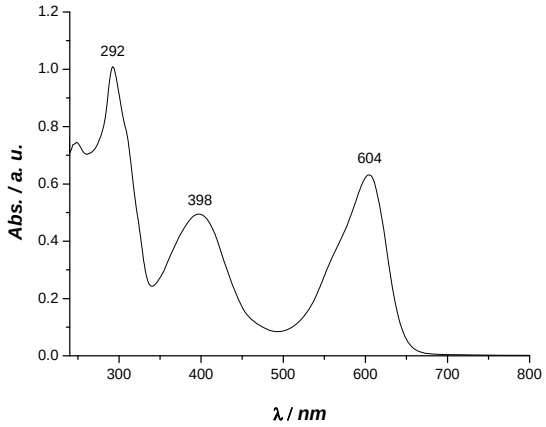

Figure 6. UV-Vis spectra of **22** (20 mg/L in NMP).

Under the polarization microscope, when applying only *one* polarizer domains ranging from blue to yellow can be observed. Upon rotating the polarizer by 90° the colour appearance of the blue and yellow domains are inverted (Figure 7), indicating that the absorption maxima belong to electronic excitation with the vectors of the transition dipole moments being oriented orthogonal. Dichroism in indigo derivatives was already reported for 6,6′-dichloroindigo in crystalline form.[22] Large and homogeneous oriented domains can easily be generated within the LC phase by preparation on treated substrates and reach dimensions not easily accessible with crystalline materials. The orientation can be frozen by rapid cooling, so that e.g. the appearance of dichroism in the LC phase might also be valuable for technical applications. The UV-Vis spectra of **8**-**13** are presented in the supporting information.

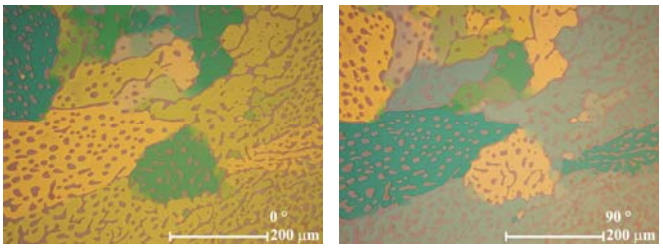

Figure 7. The liquid crystalline phase of **22** at 260°C with only one polarizer horizontal (left) and vertical (right) exhibits strong dichroism.

The *N,N*′-diacetylated, 6,6′-bis-alkylphenyl substituted **23** leads to a different phase sequence as well as a lower clearing temperature, compared to its alkoxy-analogue **13**. At 99.2°C a phase transition into a soft crystalline phase SC2 was detected, which manifests in a paramorphic “quasi fingerprint texture” when cooling from the upper SmA phase. Such a texture is known from the soft crystalline E phase, but at this stage of investigation a definite assignment cannot be given. The SmA phase of **23** was identified with PM and conoscopy observing an identical appearance as the SmA phase of **13**.

The corresponding laterally fluorinated or methylated compounds **24** and **25** exhibit complementary properties with respect to their *N,N*′-unsubstituted analogues, but also with respect to each other. The crystalline phase of the lateral methylated compound **25** shows a much higher stability compared to the laterally fluorinated compound **24**, which is the opposite case as observed for the *N,N*′-unsubstituted analogues. The methylated indigo derivative **25** melts directly into the isotropic phase at 198.0°C without the previous formation of a liquid crystalline phase. The lateral methyl group even stabilizes the crystalline phase by approximately 20°C compared to the compound **13** bearing no lateral substituent.

The fluorinated compound **24** shows a phase transition at 140.7°C into the SmA phase followed by a transition at 145.9°C into the nematic phase, which clears at 149.3°C. Both phase types have been identified by characteristic textures observed by PM. The SmA phase shows a fan like texture and has an identical appearance as described for **13**. The nematic phase exhibits a schlieren texture including singularities with the disclination strength of s = ±½ and s = ±1. The phase assignments were confirmed by wide angle X-ray scattering (WAXS). Additionally the order parameter S for each phase type could be obtained from the intensity profile of the wide angle area according to the method of Davidson et al. (see supporting information).[23]

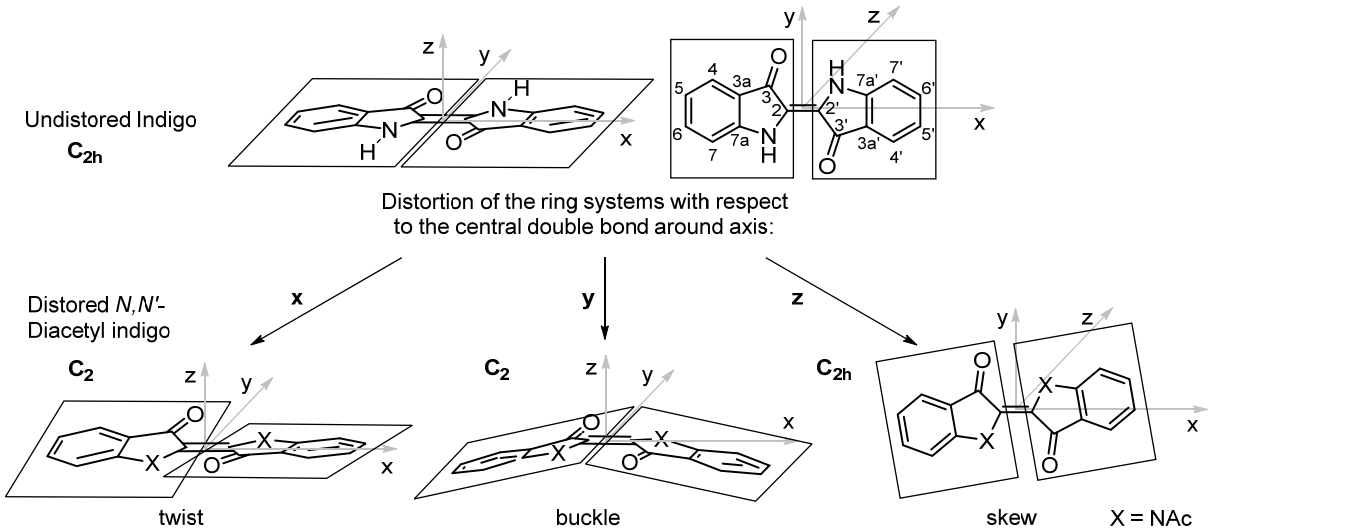

Figure 8: Rotational distortions of the ring systems with respect to the central double bond induced by *N,N'*-disubstitution of the indigo motive. When the molecule is positioned in the centre of the xy-plane with the double along the x-axis a rotational distortion around the x-axis causes a twist (left), around the y-axis a buckle and around the z-axis a skew (right). Whereas for the twist and the buckle the symmetry point group is reduced from C_{2h} to C_2, it is retained C_{2h} for the skew as this distortion is along the C_2-axis of the molecule.

The nematic phase of **24** possesses a value S=0.47 at 148°C, which is within the typical range of the nematic phase. The determined order parameter for the SmA-phase is S=0.55 at 144°C, which is unusually low.[24] This is most likely a result of the bent shape of the distorted *N,N'*-diacetyl indigo core which is discussed in more detail below.

Conformational Aspects

For the examined *N,N'*-diacetylated compounds liquid crystalline behaviour was exclusively found with a substitution pattern in the 6 and 6' positions. In order to gain insight into the origins of this observation, the inherent molecular distortions of *N,N'*-diacetyl indigo in general were analysed and in a later step compared to those of the peripherally bis-substituted *N,N'*-diacetyl indigos **12** and **23**.

When the planar indigo molecule is *N,N'*-disubstituted, the ring systems, which are connected by the central double bond, experience rotational distortions in all three spatial dimensions with respect to the double bond as illustrated in Figure 8.

It is known that *N,N'*-disubstitution of indigo leads to a buckling and twisting of the central double bond. This phenomena is caused by the steric demand of the substituent and was first observed for *N,N'*-dimethyl indigo,[25] but appears in more pronounced form in *N,N'*-diacetyl indigo. The buckling is a direct result of the twist of the central π-bond, since the sp2 orbitals of the bonded atoms rehybridise with a higher p-character (sp^n, with 2<n<3), which leads to a pyramidalisation of the bond geometry. Origins of the skew are different bond lengths and pyramidalisations for different atoms within each ring system.

Because buckling and twisting are interrelated to each other it is nontrivial to separately describe these distortions as required for a quantitative comparison between different *N,N'*-diacetylated indigos. A powerful tool was found in the p-orbital axis vector (POAV) analysis, as introduced by Haddon *et al.*[26] In the POAV1 theory the p-orbital axis vector is defined to have equal angles $\Theta_{\sigma\pi} \geq 90°$ to all three σ-bonds. $\Theta = \Theta_{\sigma\pi}-90°$ precisely quantifies the pyramidalisation from which the $s^m p$ hybridization and the average sp^n hybridization may be calculated. The degree of pyramidalisation of the C2-atom $\Theta_{C2} = \Theta_{\sigma\pi(C2)}-90°$ is a direct measure for the buckling of the molecule.

However, in the POAV1 theory an equal σ-bond hybridization in C_{3v} symmetry is assumed, which may lead to significant deviations of the actual hybridization, when the bond angles Θ_{ij} to the surrounding atoms substantially differ. This case is given for the here examined indigoid structures and a more precise description of the axis vector and the s^mp-hydridisation is then obtained from the POAV2 theory which treats the σ-bond hybridizations individually.[27] The dihedral angle $\Theta_{\pi\pi}$ between two POAVs accurately designates the π-orbital alignment and the actual twist within the molecule and is separated from the buckling distortion. The torsion angle $\Theta_{C2\text{-}C2'}$ precisely quantifies the twist of the indigo motif. Details on the performed calculations of the POAVs are given in the supporting information. The angle σ is defined as the angle between two lines, one passing through the centre of C5/C6 and the centre of C5'/C6', the other one passing through C2 and C2'. This angle σ specifies the lateral skew of the ring systems with respect the central double bond. It is defined to be σ > 0 when the ring systems are shifted in a direction in which the atoms C5 and C5' are more in line with the central double bonds than C6 and C6'.

Additionally, four further characteristic angles were determined. The effective ring twist α describes the torsion between the ring systems and is defined as the dihedral angle of C5 - C6 - C6' - C5'. This twist originates from the torsion $\Theta_{C2\text{-}C2'}$ of the central double bond but may be altered in magnitude by compensation or amplification due to further internal twists within the ring systems. β_{C5} is defined as the angles between

two lines, one passing through the C5 carbon atom and the opposing C7a atom in the same phenyl ring, the other one passing through the C5′ and the C7a′ of the phenyl ring on the other side of the central double bond. β_{C6} is correspondingly defined for lines passing through C6 and C3a on the one side and C6′ and C3a′ on the other side. These angles can have values from 0° for parallel alignment to 90° for orthogonal alignment and serve as a measure of the bent of the indigoid structure with respect to the corresponding substitution position 5 and 6. The overall bent γ is defined as the sum of two angles each between two lines. The central line is passing through C2 and C2′. The plane lines are connecting the centre of C5/C6 and centre of C3a/C7a on the one ring system and the centre of C5′/C6′ and centre of C3a′/C7a′ on the other ring system. The sum of the angle between the central line and each plane line describes the position unspecific bent of the molecule. The plane lines are on the same plane as the lines used to define β_{C5} and β_{C6} which allows comparing these different measures for the bent directly.

Computational Results

The molecular geometry of *N,N*′-diacetyl indigo obtained from X-ray diffraction was discussed and compared to quantum mechanical calculations on the AM1-SCF-level by Grimme *et al*.[28] However, in this discussion different angle definitions were applied. The C_2-symmetric molecular shape of this calculated structure is in accordance with the overall molecular geometry found from the X-ray diffraction, but shows strong deviations with respect to the magnitude of the angles. Therefore, we decided to recalculate the molecular geometry using the more recent B3LYP density functional[29] and the 6-311G(d)-basis set, as implemented in the Gausian 03[30] package (see supporting information). Though in the crystal structure solely the C_2-symmetric species was found, we also considered an alternative Ci-symmetric molecular geometry in our calculations, which also minimizes the steric strain and in principle may exist in solution or fluid phase. In such a C_i-symmetric conformation the pyramidalisation Θ is of opposing algebraic sign for C2 and C2′, thus the angle of torsion $\Theta_{(C2\text{-}C2')}$ of the ring systems is 180°, which leads to a step-like arrangement. Both possible geometries were found as local energetic minima and are shown in Figure 9. However, the difference of the sum of electronic and zero point energies of both the C_2- and C_i-symmetric conformations was computed to be ΔH=32.1 kJ/mol, favouring the C_2-symmetric conformer. Thus the existence of the C_i-symmetric conformer in solution or a fluid phase can be neglected.

The calculated and experimental results are summarized in Table 4. The stepwise arrangement of the two ring systems in the C_i-symmetric conformer only allows a relief of the steric strain of the *N*-acetyl bond of 38.4° by an extremely high torsion $\Theta_{(N\text{-}C8)}$. As a result here the most dominant pyramidalisations are found for N and C8, whereas the pyramidalisations for C2 and C3 are significantly lower than in the C_2-symmetric conformation. The inversion symmetry of the C_i-conformer implies opposing algebraic signs for each ring system, hence an effective ring twist α and an overall bent γ of zero. Consequently, β_5 and β_6 are zero, indicating a parallel alignment for each set of lines. The seemingly high skew of σ = 11.63° is an artefact caused by its definition, since for a stepwise alignment it determines the magnitude of the step and not the lateral skew. Other possible definitions as for instance the dihedral angle between the centre of C5/C6, the centre of C5′/C6′, C2′ and C2 indicate a skew of 0°.The situation is very different for the C_2-symmetric conformer, resulting from the combination of the distortions twist, buckle and skew in all three spatial dimensions. In this conformer the ring systems of the indigo structure are distorted in a disrotatory way by the twist and buckle deformation, but in a conrotatory way for the skew deformation.

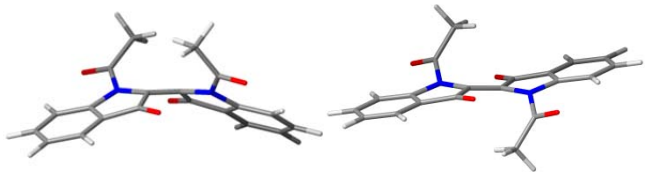

Figure 9. Calculated geometries of *N,N*′-diacetyl indigo in the actual C_2-symmetry (left) and the hypothetical C_i-symmetry (right).

For the sake of clarity it is helpful to first describe the effect of each distortion separately. The torsion of the central double bond by Θ just by itself twists the ring planes, such that $\Theta = \alpha$, since the defined peripheral bond vectors of the dihedral angle are perpendicular to the rotational axis. In this case the 5 and 5′ positions migrate to the opposite face of the central double bond than the 6 and 6′ positions.

The magnitude of β_5 and β_6 is identical, but smaller than Θ, as the defining lines are not perpendicular to the axis of rotation. The overall bent γ would stay zero for only a twist deformation since all lines are along the rotational axis. The buckling of the C_2-symmetric conformer is a result of the pyramidalisation of C-2 and C-2′ by Θ and Θ', respectively, with identical algebraic signs. Therefore, the buckling without twist or skew would lead to a bending of the central double bond, leaving the 5, 5′, 6 and 6′ positions in the same plane, parallel to the double bond, resulting in $\alpha = 0$ and $\beta_{C5} = \beta_{C6}$. The overall bent γ would be more acute than β_{C5} and β_{C6} as line between the centres of C5/C6 and C3a/C7a runs perfectly perpendicular to the axis of distortion, while the defining lines β_5 and β_6 of are not. The skew deformation by itself leaves both ring systems on the same plane, thus the effective ring twist α stays zero. As the ring systems are rotated conrotatory the defining lines for β_{C5} and β_{C6} each stay parallel, hence $\beta_{C5} = \beta_{C6} = 0$. The defining angles for the overall bent γ are of the same magnitude, but of opposing algebraic signs and will cancel out, resulting in $\gamma = 0$.

As indicated in Figure 8 the deformations twist and buckle, by itself, result in a chiral C_2-symmetric conformer. By inverting the algebraic sign of either Θ and Θ' or Θ the enantiomer of the respective conformation is formed. Since enantiomers are energetically degenerated, there is no directional preference for the bending or the torsion of the double bond.

Table 4. Comparison of characteristic angles and distances of *N,N'*-diacetyl indigo obtained by X-ray diffraction and DFT-computation applied to the C_2- and C_i-symmetric conformers.

	C_i-symmetry (DFT calc.)	C_2-symmetry (DFT calc.)	*N,N'*-diacetyl indigo (exp.)[28]
$\langle\Theta_{C2}\rangle$ [a] [°] / m [b]	±1.71 / 0.002	5.44 / 0.017	5.90 / 0.020
$\langle\Theta_{N}\rangle$ [a] [°] / m [b]	±7.07 / 0.029	3.91 / 0.009	5.99 / 0.021
$\langle\Theta_{C3}\rangle$ [a] [°] / m [b]	±0.23 / 0.000	1.35 / 0.001	1.72 / 0.002 [c]
$\langle\Theta_{C8}\rangle$ [a] [°] / m [b]	±2.77 / 0.005	1.85 / 0.002	1.36 / 0.001
$\Theta_{(C2\text{-}C2')}$ [b] [°] / $d_{C2\text{-}C2'}$ [Å]	180.00 / 1.362	-24.15 / 1.364	-19.37 / 1.349
$\langle\Theta_{(C2\text{-}C3)}\rangle$ [b] [°] / $\langle d_{C2\text{-}C3}\rangle$ [Å]	±11.64 / 1.514	12.44 / 1.509	13.87 [c] / 1.501
$\langle\Theta_{(C2\text{-}N)}\rangle$ [b] [°] / $\langle d_{C2\text{-}N}\rangle$ [Å]	±159.12 / 1.413	162.06 / 1.407	157.67 [c] / 1.414
$\langle\Theta_{(N\text{-}C8)}\rangle$ [b] [°] / $\langle d_{N\text{-}C8}\rangle$ [Å]	±38.40 / 1.438	-21.02 / 1.424	-20.49 [c] / 1.411
σ Ln (5/6-5′/6′) to Ln (2-2′) [°]	11.63	4.28	7.37
$\alpha_{(C5\text{-}C6\text{-}C6'\text{-}C5')}$ [°]	0.00	-24.67	-19.17
β_{C5} = Ln (5-7a) to Ln (5′-7a′) [°]	0.00	49.14	52.90
β_{C6} = Ln (3a-6) to Ln (3a′-6′) [°]	0.00	23.45	32.44
γ = Ln (5/6-3a/7a) to Ln (2-2′) + Ln (5′/6′-3a′/7a′) to Ln (2-2′) [°]	0.00	43.65	51.44 [c]

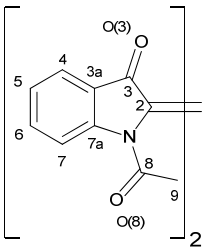

Θ_X denotes the angle of pyramidalisation of the atom X, m the degree of s-character of the s^mp hybrid orbital, $\Theta_{(X\text{-}Y)}$ the dihedral angle between the s^mp-orbitals of the two neighbouring atoms X and Y and $d_{X\text{-}Y}$ the distance between X and Y. Pointy brackets indicate the average value from both sides of the central double bond. "Ln" denotes a line which was defined to pass through the specified atoms. The angle between the lines was determined using the Diamond 3 software from *Crystal Impact*. The notation X/Y indicates that a dummy atom at the centre between atom X and Y was used. [a] obtained from POAV1 analysis, [b] obtained from POAV2 analysis, [c] significant asymmetry. A detailed list of all the calculated parameters is given in the supporting information.

The conformers, that result when twisting and buckling occur together, still retain C_2-symmetry, because the C_2-axis for both, singly distorted conformers are identical, but now are diastereomeric. The buckling in one direction energetically discriminates the direction of the twist and vice versa. In the preferred conformation the acetyl groups are on the convex face of the molecule, due to the reduction of steric strain. Thus the 5 and 5′ positions, which are para relative to the amide groups, are pushed towards the concave molecular face. While the degrees of the effective ring twist α and the overall bent γ stay nearly unaffected by the combination of these distortions, there is now a substantial difference between β_{C5} and β_{C6}, since the angle between the lines defining β_{C5} are now more acute than the overall bent γ and the lines defining β_{C6} are now less acute. Just considering the twist and the buckle deformation the difference between γ and each β angle should be identical. However, the positive skew rotates the ring systems in a way that the positions 5 and 5′ are more in line with the central double bond, which shifts up the ring systems on their planes and decreases both β_{C5} and β_{C6}, while leaving the overall bent γ nearly unaffected. Thus the position specific molecular bending β_{C5} is now only slightly higher than γ, whereas the position specific molecular bending β_{C6} is significantly reduced compared to γ. As a result 5,5′-bis-substituted *N,N*′-diacetyl indigo derivatives show high molecular bents and are not suitable for the formation of mesophases, whereas the 6,6′-bis-substituted *N,N*′-diacetyl indigo derivatives are much less bent. The molecular shape of the latter derivative is still not ideal rod-like, but within the window of calamitic mesogens. Deviations in magnitude from this general trend are caused by further internal distortions within each ring system.

Though the DFT-calculation of the C_2-symmetric conformer gives much better results than obtained by the AM1-SCF-method, it can be seen that the pyramidalisation Θσπ and the s-character of the s^mp hybrid orbital of the atoms C2, C3 and especially N are generally underestimated, when compared to the crystal structure, whereas Θ_{C8} is slightly overestimated. On the other hand the torsion $\Theta_{(C2\text{-}C2')}$ of the central π-bond was predicted to be 4.8° higher than actually found, which is also reflected in the difference of the bond lengths, whereas the average torsion $\langle\Theta_{(C2\text{-}N)}\rangle$ was computed to be smaller by 4.4°. It has to be mentioned that due to crystal packing effects the these average torsions angles show significant asymmetric deviations of 7-12°, however the more consistent bond length substantiate this trend.

The most significant deviations were found in connection to the nitrogen atom. It seems that the steric strain, which is induced by the acetyl groups, is stronger compensated by the N pyramidalisation Θ_N and the torsion $\Theta_{(C2\text{-}N)}$ than predicted. This allows a less twisted central π-bond and a higher degree of conjugation between the two ring systems. On the other hand, due to the higher distortion of the nitrogen bonds the skew angle σ is significantly increased by 3.1°, when compared to the computed gas phase structure. For both cases, the computed and the measured structure, the effective ring twist α very accurately reflects torsion $\Theta_{(C2\text{-}C2')}$ of the central π-bond. The overall bent γ – and thus β_{C5} and β_{C6} – was found to be substantially higher for the crystal structure than predicted for the gas phase. However, in the crystal structure the two angles contributing to γ, one for each ring system, largely differ with 34.5° and 16.9°, indicating strong crystal forces. The higher value was found for the ring system with the stronger pyramidalisation of atoms.

Crystal Structures

For the peripherally bis-substituted compounds **12** and **23** it was possible to obtain crystals suitable for single crystal X-ray diffraction. Figure 10 and Figure 11 show two projections of the molecular structures of **12** and **23**, respectively.

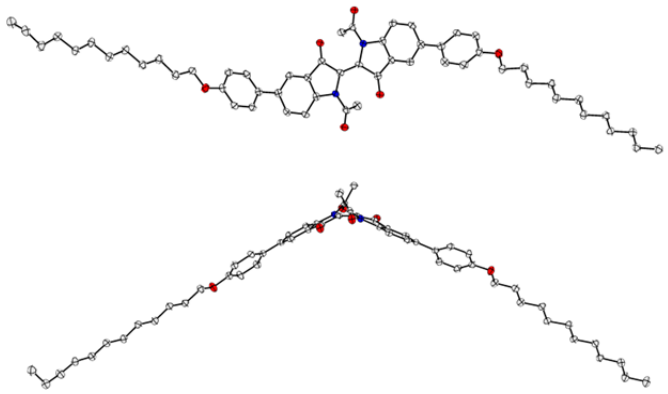

Figure 10. Structure of the 5,5′-bis-substituted compound **12** in the solid state, shown in two projections. The anisotropic displacement parameters are drawn at the 50% probability level. Oxygen atoms are drawn in red; nitrogen atoms in blue. Only one crystallographic type of molecule was observed.

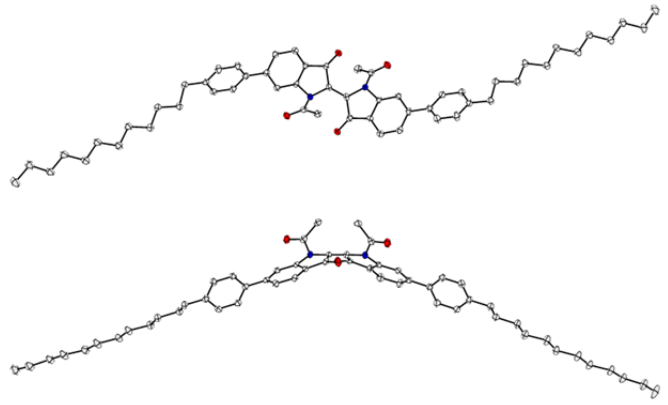

Figure 11. Molecular structure of the 6,6′-bis-substituted compound **23** as found in the crystalline state, shown in two projections. The anisotropic displacement parameters are drawn at the 50% probability level. Oxygen atoms are drawn in red; nitrogen atoms in blue. Only one crystallographic type of molecule was observed.

Like in the unit cell of the parent structure *N,N*′-diacetyl indigo only one crystallographic type of molecule was found as a racemate of conformers in both crystal structures. However, **23** was crystallized from NMP and crystal structure still contains two molecules of NMP per molecule **23** with one them being disordered.

It is known for anilines that electron withdrawing substituents decrease the pyramidalisation of the nitrogen due to an increased donor-acceptor conjugation between the nitrogen lone pair and the substituent. This effect is strongest for para-substitution, but prevails to a lesser extent for meta-substituents.[31] Electron pushing substituents as 4-alkylphenyl or 4-alkoxyphenyl show the opposite effect. In order to estimate if the different distortions of **12** and **23** found in their crystal structures originate from the altered substitution pattern or from crystal packing effects, the geometries of a set of correspondingly substituted *N,N*′-diacetyl indigo structures was computed using the same DFT-method as described above (see supporting information). With regard to the computational effort the chain length of the substituent was reduced to 4-ethylphenyl (PhEt) and 4-methoxyphenyl (PhOMe).

In Table 5 the experimentally determined molecular geometries of **12** and **23** are compared to the computed structures. The C2 pyramidalisation Θ_{C2} is in good accordance for all structures, slightly increased for **12**. The torsion $\Theta_{(C2\text{-}C2')}$ of the central double bond shows a high conformity in all experimentally determined geometries, but seems to be systematically overestimated by 4-5° in the computed structures. Substantial differences were found for the parameters, which are associated with the nitrogen atom and the acetyl group. Compared to the unsubstituted *N,N*′-diacetyl indigo structure the pyramidalisation Θ_N of the nitrogen atom is strongly decreased for the 5,5′-bis-substituted **12**, whereas it is significantly increased for the 6,6′-bis-substituted **23**, also indicated by the higher torsion $\Theta_{(C2\text{-}N)}$ between the nitrogen and the neighbouring carbon of the central π-bond. This finding could be explained by the conjugation between the electron pushing substituent in position 5 with the *N*-acetyl group in the same ring system as well as the N-acetyl and the carbonyl group of the opposing one – all involving the nitrogen atoms. A conjugation for substituent in position 6 only occurs with the carbonyl group of the same ring system, leaving the nitrogen atom unaffected. The computed geometries of correspondingly substituted confirm this trend but to a diminished extent indicating strong crystal forces. In **12** the steric strain induced by the acetyl groups is mainly compensated by a high torsion $\Theta_{(N\text{-}C8)}$ between nitrogen atom and the carbon of the acetyl group, whereas **23** shows much lower values for these torsions. The position specific bent angles β_{C5} and β_{C6} of **12** are in good accordance with those of the computed structures. In **23**, on the other hand, the stain seems to be compensated to a higher extent by internal distortions of the ring systems causing them to be less twisted against each other but generally more bent than **12**, as indicated by values for α and γ. Both β_{C5} and especially β_{C6} of compound **23** are higher than predicted computationally. All computed structures show independently of their substitution pattern only little deviation among each other for all determined parameters. Thus, it is very likely that the strong distortions found in **23** rather originate from crystal effects than from its substitution pattern. The value for β_{C6} of **23** in the fluid phase may therefore be expected lower than found in the crystal structure.

The observed bent angle of approximately 130° for the 5,5′-bis-substituted indigo derivatives is within the suitable range for bent-core mesogens.[32] However, these phases were not observed for the compounds presented in this article. The 6,6′-bis-substituted indigo derivatives have a more obtuse bent angle of approximately 150°. Bent angles around 150° are considered to be on the border between calamitic and bent core mesogens.

Table 5. Comparison of the experimentally determined characteristic angles and distances of compounds 12 and 23 as well as the computed values for 5,5′- and 6,6′-bis-substituted *N,N*′-diacetyl indigo compounds with 4-ethylphenyl (PhEt) and 4-methoxyphenyl (PhOMe) substituents.

	12 (5,5′)	**23** (6,6′)	5,5′-DiPhEt	5,5′-DiOMe	6,6′-DiPhEt	6,6′-DiOMe
	Exp.	Exp.	Calc.	Calc.	Calc.	Calc.
Space group	$P2_1/n$	$P2_1/c$				
$\langle\Theta_{C2}\rangle^{[a]}$ [°] / m[b]	6.18 / 0.022	5.57 / 0.018	5.52 / 0.017	5.44 / 0.017	5.43 / 0.017	5.37 / 0.016
$\langle\Theta_{N}\rangle^{[a]}$ [°] / m[b]	2.72 / 0.004[c]	8.83 / 0.047	3.84 / 0.008	3.89 / 0.009	4.22 / 0.010	4.26 / 0.010
$\langle\Theta_{C3}\rangle^{[a]}$ [°] / m[b]	1.62 / 0.001	1.58 / 0.001	1.33 / 0.001	1.37 / 0.001	1.38 / 0.001	1.37 / 0.001
$\langle\Theta_{C8}\rangle^{[a]}$ [°] / m[b]	2.34 / 0.003	1.33 / 0.001[c]	1.83 / 0.002	1.75 / 0.002	1.73 / 0.002	1.78 / 0.002
$\Theta_{(C2\text{-}C2')}^{[b]}$ [°] / $d_{C2\text{-}C2'}$ [Å]	-19.46 / 1.362	-19.71 / 1.351	-24.60 / 1.364	-24.53 / 1.364	-24.30 / 1.363	-23.69 / 1.363
$\langle\Theta_{(C2\text{-}C3)}\rangle^{[b]}$ [°] / $\langle d_{C2\text{-}C3}\rangle$ [Å]	12.44 / 1.499	15.21 / 1.500	12.44 / 1.510	12.11 / 1.510	12.66 / 1.510	12.47 / 1.510
$\langle\Theta_{(C2\text{-}N)}\rangle^{[b]}$ [°] / $\langle d_{C2\text{-}N}\rangle$ [Å]	163.80 / 1.413	153.82 / 1.418	162.10 / 1.407	162.33 / 1.407	161.55 / 1.409	161.57 / 1.409
$\langle\Theta_{(N\text{-}C8)}\rangle^{[b]}$ [°] / $\langle d_{N\text{-}C8}\rangle$ [Å]	-31.52 / 1.419	-17.18 / 1.412	-20.48 / 1.423	-20.75 / 1.422	-20.06 / 1.422	-20.55 / 1.422
σ = Ln (5/6-5′/6′) to Ln (2-2′) [°]	3.91	5.86	4.20	4.06	4.69	4.59
$\alpha_{(C5\text{-}C6\text{-}C6'\text{-}C5')}$[°]	-26.05	-18.68	-26.08	-25.80	-23.95	-22.59
β_{C5} = Ln (5-7a) to Ln (5′-7a′) [°]	50.60	54.29	49.97	48.54	50.07	49.01
β_{C6} = Ln (3a-6) to Ln (3a′-6′) [°]	26.11	32.41	23.83	22.74	24.04	24.13
γ = Ln (5/6-3a/7a) to Ln (2-2′) + Ln (5′/6′-3a′/7a′) to Ln (2-2′) [°]	45.71	52.90	44.29	42.75	44.79	44.20

Θ_X denotes the angle of pyramidalisation of the atom X, m the degree of s-character of the $s^m p$ hybrid orbital, $\Theta_{(X\text{-}Y)}$ the dihedral angle between the $s^m p$-orbitals of the two neighbouring atoms X and Y and $d_{X\text{-}Y}$ the distance between X and Y. Pointy brackets indicate the average value from both sides of the central double bond. "Ln" denotes a line which was defined to pass through the specified atoms. The angle between the lines was determined using the Diamond 3 software from *Crystal Impact*. The notation X/Y indicates that a dummy atom at the centre between atom X and Y was used. [a] obtained from POAV1 analysis, [b] obtained from POAV2 analysis, [c] significant asymmetry. A detailed list of all the calculated parameters is given in the supporting information.

In this context the unusual low order parameter found for the SmA phase of **24** can be understood as the higher degree of disorder caused by this bending. Such low bent angle mesogens have gained much attention recently, due to high tendency to form uncommon phases types, such as the $SmAP_A$[33] or the $SmAP_R$.[34] By introduction of flexible linking groups such as esters or imines, bent core liquid crystalline phases may be induced. Such a sterically deformed π-system could serve as an unusual and unique bent unit and will be subject of further investigation.

The peripheral substitution pattern also has a tremendous influence on the kinetics of the trans-cis-photoisomerization of the *N,N*′-diacetylated indigo derivatives. Substitution in the 5 and 5′ positions leads to a decrease in the rate of the isomerization compared to *N,N*′-diacetyl indigo. The cis-product could not be observed even under long and intense exposure to light. In contrast the substitution in the 6 and 6′ positions leads to a considerable increase of the isomerization rate. The cis-product was observed after short time exposure to sunlight indicating an increase of the quantum yield for the isomerization process compared to *N,N*′-diacetyl indigo. This phenomenon could be exploited to generated new photoresponsive materials.

Conclusion

We presented an efficient synthesis for a wide spectrum of peripherally substituted indigo derivatives. Substitution at the 4,4′ and 7,7′ positions lead to a considerable increase in solubility, which presumably originates from steric hindrance of intermolecular H-bonding.

The *N,N*′-unsubstituted compounds, bearing pendant groups in the 5,5′ and 6,6′ positions possess an approximately rod like molecular shape. Low solubility and high melting temperature, caused by H-bonding, dominate their thermotropic behaviour, as they are characteristic for indigo. The 5,5′-bis-substituted derivatives exhibit liquid crystalline phases only shortly before or during decomposition. Stable, highly ordered smectic phases were found for the derivatives substituted with laterally fluorinated or methylated pendant groups at 6 and 6′ positions. For these phases a pronounced dichroism was observed.

Upon acetylation of the vinylogue amide groups the solubility of all indigo derivatives was increased and the melting temperatures were reduced. LC phases, however, were exclusively found for the compounds substituted at the 6 and 6′ positions. Based on a structural analysis of *N,N*′-diacetyl indigo it is supposed that the combination of buckling and twisting of the central double bond leads to molecular bent which is specific for the substitution position. For 6,6′-bis-substituted *N,N*′-diacetyl indigos, the molecular bent is reduced compared to the bent of the core system, whereas it is amplified for the substitution positions 5 and 5′.

Acknowledgements

We gratefully acknowledge Prof. F. Gießelmann for allowing us the access to his X-ray facilities for diffraction on LCs, Prof. Schwarz for respective devices for single crystal X-ray measurements, and M. Moran and R. Callahan for fruitful discussions.

Notes and references

1 1. a) O. Ostroverkhova and W. E. Moerner, *Chem. Rev.*, 2004, **104**, 3267-3314; b) D. M. Burland, R. D. Miller and C. A. Walsh, *Chem. Rev.*, 1994, **94**, 31-75; c) F. Kajzar, K.-S. Lee and A. K.-Y. Jen, eds., *Polymers for Photonics Applications II* Springer, Berlin, 2003.

2 2. a) L. Schmidt-Mende, A. Fechtenkötter, K. Müllen, E. Moons, R. H. Friend and J. D. Mackenzie, *Science*, 2001, **293**, 1119-1122; b) S.-S. Sun and N. S. Sariciftci, *Organic Photovoltaics - Mechanism, Materials and Devices*, CRC Press, Boca Raton, FL, 2005; c) L. Li, S. W. Kang, J. Harden, Q. Sun, X. Zhou, L. Dai, A. Jakli, S. Kumar and Q. Li, *Liq. Cryst.*, 2008, **35**, 233-239.

3 3. a) H. P. Preiswerk, M. Lubanski and F. K. Kneubühl, *Appl. Phys. B: Laser Opt.*, 1984, **33**, 115-131; b) S. M. Morris, M. M. Qasim, D. J. Gardiner, P. J. W. Hands, F. Castles, G. Tu, W. T. S. Huck, R. H. Friend and H. J. Coles, *Opt. Mater.*, 2013, **35**, 837-842.

4 4. a) K. Ariga and T. Kunitake, *Supramolecular Chemistry - Fundamentals and Applications*, Springer Verlag, Berlin Heidelberg New York, 2006; b) V. Balzani, *Tetrahedron*, 1992, **48**, 10443-10514; c) H. K. Bisoyi and Q. Li, *Acc. Chem. Res.*, 2014, **47**, 3184-3195.

5 5. C. A. Mirkin and M. A. Ratner, *Annu. Rev. Phys. Chem.*, 1992, **43**, 719-754.

6 6. S. Kundu, T. Ray, S. K. Roy and S. S. Roy, *Jap. J. Appl. Phys.*, 2004, **43**, 249-255.

7 7. S. J. Cowling, C. Ellis and J. W. Goodby, *Liq. Cryst.*, 2011, **38**, 1683-1698.

8 8. H. Kang, J. Hong and D. Kang, *Mol. Cryst. Liq. Cryst.*, 2014, **605**, 103-116.

9 9. H. Zhang, J. Zhang and B. Tieke, *Polym. Chem.*, 2014, **5**, 646-652.

10 10. a) Z. Chen, V. Stepanenko, V. Dehm, P. Prins, L. D. A. Siebbeles, J. Seibt, P. Marquetand, V. Engel and F. Würthner, *Chem.--Eur. J.*, 2007, **13**, 436-449; b) X. Li, A. Liu, S. Xun, W. Qiao, X. Wan and Z. Y. Wang, *Org. Lett.*, 2008, **10**, 3786-3787; c) L. Marin, A. Zabulica and M. Sava, *Soft Materials*, 2013, **11**, 32-39.

11 11. M. Klessinger and W. Lüttke, *Tetrahedron*, 1963, **19, Suppl. 2**, 315-335.

12 12. a) R. Wizinger, *Chimia*, 1961, **15**, 89-105; b) R. Grinter and E. Heilbronner, *Helv. chim. Acta*, 1962, **45**, 2496; c) H. Labhart and Wagnière, *Helv. chim. Acta*, 1963, **46**, 1314-1326; d) W. Lüttke and M. Klessinger, *Chem. Ber.*, 1964, **104**, 2342-2357.

13 13. a) A. v. Baeyer, *Ber. Dtsch. Chem. Ges.*, 1878, **11**, 1296-1297; b) A. v. Baeyer, *Ber. Dtsch. Chem. Ges.*, 1879, **12**, 456-461.

14 14. A. R. Katritzky, W.-Q. Fan, A. E. Koziol and G. J. Palenik, *J. Heterocycl. Chem.*, 1989, **26**, 821-828.

15 15. J. H. Porada and D. Blunk, *J. Mater. Chem.*, 2010, **20**, 2956-2958.

16 16. D. Blunk and J. H. Porada, *Chemphyschem*, 2009, **10**, 3260-3264.

17 17. P. Süsse, M. Steins and V. Kupcik, *Z. Kristallogr.*, 1988, **184**, 269.

18 18. C. Liebermann and F. Dickhuth, *Chem. Ber.*, 1891, **24**, 4130-4136.

19 19. a) J. E. Klare, G. S. Tulevski, K. Sugo, A. de Picciotto, K. A. White and C. Nuckolls, *J. Am. Chem. Soc.*, 2003, **125**, 6030-6031; b) N. Lindner, M. Kölbel, C. Sauer, S. Diele, J. Jokiranta and C. Tschierske, *J. Phys. Chem. B*, 1998, **102**, 5261-5273; c) G. W. Gray, C. Hogg and D. Lacey, *Mol. Cryst. Liq. Cryst.*, 1981, **67**, 1-23.

20 20. M. C. Carreño, J. L. García Ruano, G. Sanz, M. A. Toledo and A. Urbano, *Synlett*, 1997, 1241-1242.

21 21. a) G. Miehe, P. Süsse, V. Kupcik, E. Egert, M. Nieger, G. Kunz, R. Gerke, B. Knieriem, M. Niemeyer and W. Lüttke, *Angew. Chem. Int. Ed. Engl.*, 1991, **30**, 964-967; b) G. A. Russell and G. Kaupp, *J. Am. Chem. Soc.*, 1969, **91**, 3851-3859.

22 22. P. Süsse and R. Wäsche, *Naturwissenschaften*, 1978, **65**, 157.

23 23. P. Davidson, D. Petermann and A. M. Levelut, *J. Phys. II France*, 1995, **5**, 113-131.

24 24. J. W. Goodby, D. Demus, J. Goodby, G. W. Gray, H. W. Spiess and V. Vill, in *Handbook of Liquid Crystals*, Wiley-VCH Verlag GmbH, 2008, pp. 3-21.

25 25. G. Miehe, P. Süsse, V. Kupcik, E. Egert, M. Nieger, G. Kunz, R. Gerke, B. Knieriem, M. Niemeyer and W. Lüttke, *Angew. Chem. Int. Ed.*, 1991, **30**, 964-967.

26 26. R. C. Haddon and L. T. Scott, *Pure Appl. Chem.*, 1986, **58**, 137-142.

27 27. a) R. C. Haddon, *Chemical Physics Letters*, 1986, **125**, 231-234; b) R. C. Haddon, *J. Am. Chem. Soc.*, 1986, **108**, 2837-2842.

28 28. G. Grimme, S. Grimme, P. G. Jones and P. Boldt, *Chem. Ber.*, 1993, **126**, 1015-1021.

29 29. a) A. D. Becke, *J. Chem. Phys.*, 1993, **98**, 5648-5652; b) C. T. Lee, W. T. Yang and R. G. Parr, *Phys. Rev. B*, 1988, **37**, 785-789; c) B. Miehlich, A. Savin, H. Stoll and H. Preuss, *Chemical Physics Letters*, 1989, **157**, 200-206.

30 30. M. J. Frisch and et al., *Journal*, 2004.

31 31. I. V. Alabugin, M. Manoharan, M. Buck and R. J. Clark, *J. Mol. Struc: Theochem*, 2007, **813**, 21-27.

32 32. R. A. Reddy and C. Tschierske, *J. Mater. Chem.*, 2006, **16**, 907-961.

33 33. I. Wirth, S. Diele, A. Eremin, G. Pelzl, S. Grande, L. Kovalenko, N. Pancenko and W. Weissflog, *J. Mater. Chem.*, 2001, **11**, 1642-1650.

34 34. a) D. Pociecha, M. Čepič, E. Gorecka and J. Mieczkowski, *Phys. Rev. Lett.*, 2003, **91**, 185501; b) Y. Shimbo, E. Gorecka, D. Pociecha, F. Araoka, M. Goto, Y. Takanishi, K. Ishikawa, J. Mieczkowski, K. Gomola and H. Takezoe, *Phys. Rev. Lett.*, 2006, **97**, 113901.

35